

Optimized Cooling Solutions for Lithium-Ion Batteries in Electric Vehicles using PCM Composites

Muthukumar Marappan^{1*}, *A Mahendran*², *G Ravivarman*³, *K Suresh Kumar*⁴, *M Elango*⁵, *S P Kesavan*⁶, and *R Devarajan*⁷

¹Department of Mechanical Engineering, Nandha Engineering College, Erode 638052, Tamil Nadu, India

²Department of Mechanical Engineering, Sona College of Technology, Salem 636005, Tamil Nadu, India

³Department of Electrical and Electronics Engineering, Karpagam Academy of Higher Education, Coimbatore 641021, Tamil Nadu, India

⁴Department of MBA, Panimalar Engineering College, Chennai 600123, Tamil Nadu, India

⁵Department of Mechanical Engineering, Erode Sengunthar Engineering College, Perundurai 638057, Tamil Nadu, India

⁶Department of Artificial Intelligence and Data Science, Muthayammal Engineering College, Rasipuram 637408, Tamil Nadu, India

⁷Department of Electrical and Electronics Engineering, Vinayaka Mission's Kirupananda Variyar Engineering College, Vinayaka Mission's Research Foundation (Deemed to be University), Salem 636308, Tamil Nadu, India

Abstract. Electric vehicles that use lithium ion (Li-Ion) batteries as an alternative to fossil fuels have emerged as a viable solution to the environmental and sustainability problems associated with these fuels. Due to their sensitivity, Li-Ion batteries have been the subject of intense heat management research for the last ten years. There are a number of ways to regulate the complicated dynamics that cause Li-Ion batteries' temperatures to rise. This work shows how to optimize the thermal management control variables using design of experiments (DOE), keeping it as the research emphasis. The variables used for optimization include the phase change materials mass denotes as X, the thermal conduction of paraffin aluminum composite denotes as Y, and the water flow rate denotes as Z. Researchers have looked at how these factors affect the rate of heat buildup in Li-Ion batteries. Studying the effect of Li-Ion battery temperature management parameters required a full factorial DOE with two repetitions. In order to evaluate the hypotheses, multivariate analysis made use of analysis of variance (ANOVA). This included controlling for both the 1st and 2nd order interface impact. All of the research factors significantly affected the increase in Li-Ion battery temperature, according to the hypothesis testing.

*Corresponding author: muthukumar.marappan@nandhaengg.org

1 Introduction

The automotive industry is currently seeing a boom in plug-in hybrid electric cars (PHEVs) and battery electric vehicles (BEVs) as a means to address sustainability and environmental concerns [1]. Researchers are focusing increasingly on lithium-ion (Li-Ion) batteries since they offer the best cycle life and highest energy density of all rechargeable batteries. In electric and hybrid vehicle applications, cathode materials with a high energy density, such as Li (NiMnCo) O and LiMPO, are preferred over LiCoO [2]. Operating temperature is said to have a significant impact on Li-Ion battery performance. Also, the main reason batteries fail is because the cathode material deteriorates within. As a function of cycling temperature, this test measures the capacity fading of Sony's LiCoO cell. At temperatures above 50°C, they found that the capacity fading was due to the loss of Li under LiCoO. The results of previous studies on thermal runaway and capacity fading were consistent with these findings [3]. For improved performance and longer battery life with Li-Ion batteries, it is essential to regulate their working temperature. Operating within a temperature range of 0 to 40°C, with a temperature distribution among cells below 5°C, allows lithium batteries to function optimally and extends their lifespan [4]. Temperature has an effect on the SOH, lifetime, and performance of Li-Ion batteries. Because thermal runaway and cell material degradation can occur at very high temperatures, this is the case. An important factor in how sensitive Li-Ion batteries are is their state of charge (SOC). Estimates of the rate of heat generation by Li-Ion cells have been derived from mathematical models in earlier research. The total heat created is comprised of the heating and the entropy shift that occurs throughout the charge and discharge cycles [5]. Computer simulations show that low SOC increases heat generation, which in turn raises the rate at which a battery cell's temperature rises. For a battery system utilized in PHEVs and BEVs, it is crucial to have an effective BTMS and to dynamically evaluate the health, life, and safety of Li-Ion batteries with an accurate and dependable state of charge (SOC) [6]. Several types of BTMS have been proposed in previous research. Thermoregulation of a battery pack containing many cylindrical cells was proven in a computer modeling investigation that made use of air cooling. However, the distribution of temperatures was messed up. Increasing the airflow rate and frequency of reversal or switching to liquid cooling are two ways to reduce temperature rise in active air-cooling. Incorporating fins into air cooling systems has increased temperature uniformity and performance [7]. Since the planned air/liquid cooling system relied heavily on aluminium, which may make heavier and more expensive battery packs a reality, the heating plate cool pipe idea was not workable. The lack of surface contact between the liquid channels and the cell body in several of the previously suggested studies on mini-channel liquid cooling makes them inappropriate for cylindrical or pouch cells [8]. Not to mention how time-consuming and costly it would be to fabricate these mini- and micro-channels. A comparable instance involving a cooling plate with micro-channels. If the discharge rate is more than 5°C, a bigger flow of coolant is required, which could cause the cooling channels to become quite pressurized and require a powerful pump [9]. A more controlled increase in temperature and more uniform heating of the cells have been accomplished with the implementation of PCM-based passive cooling for Li-Ion batteries. It is optimal for the PCM material to have a melting point lower than 45°C. Cooling with only PCMs is simple and effective in limiting temperature rise, but its heat dissipation efficiency is poor [10]. During repeated charging and discharging cycles, the heat would be retained within the PCM mass owing to its lack of thermal conduction. Rather than using pure PCM, composites containing PCM and graphite were created to improve thermal conductivity temperatures [11]. For the purpose of testing metal foam with pure PCM, we used aluminium and aluminum as metals. For the most part, earlier research used a 10A cell with a maximal discharge at 5C. However, when power demands increase, PCM-metal composites may not be as efficient as they are when used with

low-capacity cells [12]. Current trends in battery technology indicate that Z-fold pouch cells outperform cylindrical and prismatic cells due to their superior heat dissipation. There is a negative correlation between thickness and thermal conductivity in prismatic and pouch cells, while the inverse is true for width and length. Therefore, for optimal temperature distribution, cooling should be applied along the length and width of the object [13]. A variety of Li-Ion batteries (LIB) was found, that are ideal for use in hybrids and electric vehicles in Table 1. The amount of heat generated during full capacity discharge will be significantly greater than what has been shown in previous experiments and simulations. So, it needs a cooling mechanism that works very well and can be improved for future use.

Table 1. Generational advancements in Li-Ion battery technology

Ti	Type of Cell	Ampere rate (Ah)	Pouch size (mm) Width × Length × Thick	Maximum discharge rate	
				Continuous	Pulse
XALT energy	F940-0001 ^b	37	225 × 225 × 9.7	8C	16C
Farasis	IMP06160230P25A	25	161 × 230 × 6	4C	7C
Targray	Lithium-ion pouch ^b	44	249 × 155 × 12	3C	10C
EiG energy	ePLBC037	37	224 × 130 × 12.6	5C	10C
Tenergy	30123	10.5	157 × 59.5 × 9.8	5C	10C
Kokam	SLPB120216216HR ^{2a}	47	226 × 227 × 12.5	12C	18C
	SLPB120216216	53	226 × 227 × 12	5C	8C
	SLPB100216216H	40	226 × 227 × 10	8C	15C

(a) Imbided Nano techniques, (b) 4C capable charging rate

The most recent development in battery thermal management is a hybrid cooling technique that combines PCM with air or liquid. By incorporating air or liquid passages into the PCM mass, heat dissipation can be enhanced and managed more efficiently. Evaluation of a A-air hybridized cooling system for Li-Ion batteries (LIB) packs by numerical analysis. A rectangular-sectioned air duct was introduced into the PCM cooling mass in his work [14]. The novel approach used PCM to cool the lower two-thirds of the LIB cell and a liquid cooling channel to cool the upper one-third. By taking both the ambient and working temperatures into account, the additional control parameters provided by a hybrid cooling system could be useful in developing a cooling system that is tailor-made for the battery pack. In this study, a hybrid cooling system was applied to a LIB pack [15]. This is a potential use case for hybrid and high-performance electric automobiles. In order to examine the different design parameters, the statistical design tool is used in a parametric analysis.

1.1 Objectives of research

Controlling the temperature and performance of the battery was largely dependent on choosing and deciding upon the values of the designed factors for the hybridized cooling system. After reviewing the literature, we settled on a set of design parameters and a range of values for them to use in building our linear regression model. A number of design parameters determine the hybrid cooling system. These include PCM mass, paraffin-metal composite thermal conductivity, coolant flow rate, coolant type, and PCM type. When it comes to keeping the temperature increase, heat dispersion, and cooling rate of battery cells under control, all of these factors play a significant role. No changes were made to the PCM type or coolant for this study. The following design characteristics were taken into account for experiments and linear regression modeling:

- Used between two successive Li-Ion cells, the mass of PCM changes with PCM thickness.

- One property of PCC that changes with the number of aluminum tubes is its thermal conductivity.
- By adjusting the pressure in the aluminum pipes, the water flow rate (WFL) can be changed.

Several researches have shown that the aforementioned characteristics affect the temperature and uniform heat dispersion of LIB. Nevertheless, this research did not systematically utilize statistical tools to study the interaction effects; instead, they presented them independently. The central emphasis of this project is a new hybridized cooling system designed specifically for LIB packs found in electric vehicles and high-performance hybrids. It is anticipated that the battery pack's operating temperature will be consistent throughout a wide variety of ambient temperatures. Consequently, we investigate the impact of various design parameters on battery temperature through their interaction utilizing DOE ideas.

2 Experimental methodology

Li-Ion batteries used in motorized vehicles are the primary subject of this study. For the heat management studies, Lithium-Ion (Li-Ion) batteries was used that have a faster charge/discharge rate. Tables 2 and 3 outline the components and specifications of the Lithium-Ion cells and modules that were investigated for this investigation.

Table 2. The properties of Li-Ion batteries.

Composition	Wt. %
Aluminum (Al)	3.6–4.0
Lithium nickel cobalt manganese oxide (Li[NiCoMn ₂]O ₂)	30–37
Polyvinylidene difluoride	1.2–2.0
Lithium hexafluorophosphate (LiPF ₆)	2.2
Plastic	7.0
Carbon (C)	19–20
Aluminium (Cu)	8.2
Organic carbonate	13.1

Table 3. Attributes of Li-Ion batteries.

Factor	EV pack	Module	Cell range
Max charging rate @ 2C (A)	240	40	20
working temperature			– 15 to 45°C
Minimum voltage (VDC)	300	30	3.0±0.03
Nominal voltage (VDC)	370	37	3.7
Capacity (Ah)	120	20	10
Energy (kWh)	36	0.60	0.03
Maximum voltage (VDC)	420	42	4.2 ± 0.03
Max continuous discharge @ 10C (A)	1200	200	100
Height (mm)		~ 165	156
Width (mm)		~ 155	66
Power (kW)	360	6	0.3
Thickness (mm)		~ 170	9
Number of cells	1200	20	1

Each cell can discharge at a 15 C-rate and produce 100 A at a minimal of 3 V, provided that the capacity is less than 10 Ah. Fig. 1 shows a battery module that has twenty Li-Ion cells with a 2S10P architecture. This module can discharge currents up to twenty amperes at thirty volts, has an energy density of 600 W/hr, and can produce 6 kW of total power. The 60 kW of power and 6 kWh of energy produced by ten of these modules linked in series

would be more than enough for any hybrid vehicle. About 0.2 kWh of energy is needed for an electric vehicle to cover a distance of 1 km [16]. A high-performance electric vehicle may be powered for about 200 km on a single charge from 60 modules linked in a 6P10S configuration that generates 120 A at 300 V and 36 kWh of energy.

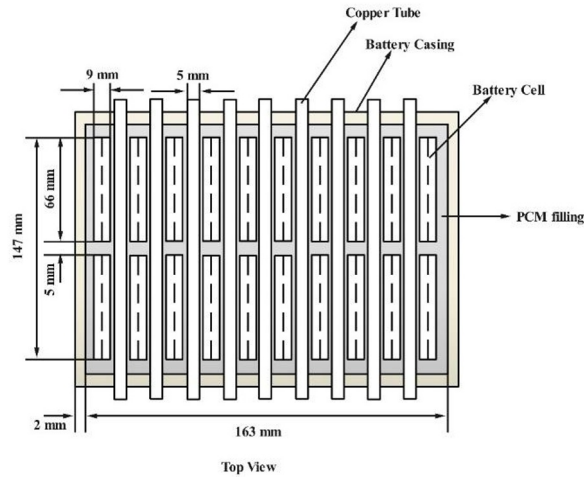


Figure 1. An improved design of the LIB module with twenty lithium-ion cells.

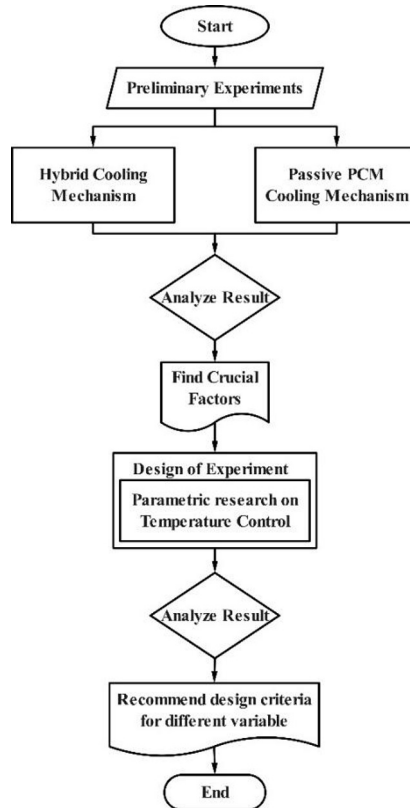


Figure 2. Flowchart of experimentation.

The whole experiment was conducted in two phases, as depicted in the flow diagram of the experiment (Fig. 2). In Stage-1, first tests were conducted with a battery module and two different cooling techniques. Between each set of Li-Ion cells, a pure PCM cooling was applied with a thickness of 10 mm. Following this, a hybrid cooling system was tested by introducing four 3/16-inch capillary aluminum tubes into the PCM cooling mass. Two liters per minute is the water circulation flow rate that was selected. The second round of trials used the "Design of Experiments" procedure to analyze the hybrid cooling system parametrically.

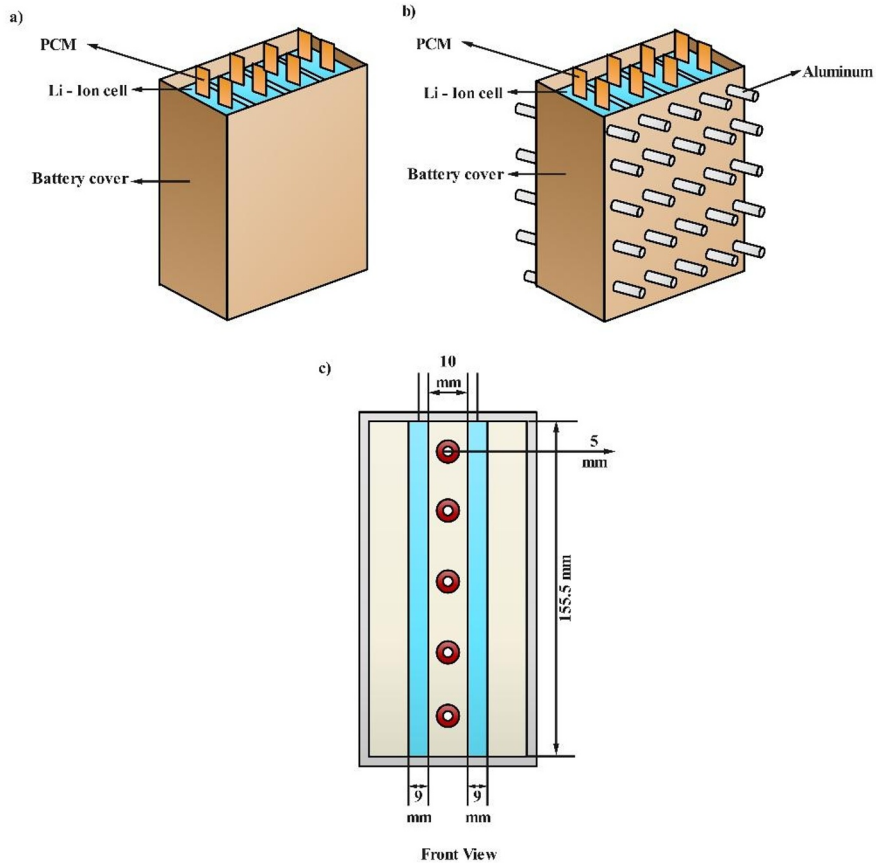


Figure 3. Mini-modules for Stage-2 investigations, hybrid cooling, and pure PCM cooling are all possible with battery modules

In Stage 2, the experimental emphasis was on a symmetrical component of the battery module, as illustrated in Fig. 3. This compact module is constructed from two Lithium-Ion pouch cells that are connected in series. Three types of battery modules on the tests were performed with 3, 5, and 7 tubes to determine the impact of the cooling mass's thermal conductivity on the results. A 20 A discharge voltage at 3.8 V and discharging rate at 1 C makes it seem like the mini module has the same electro-thermal characteristics as the big module. The present studies involved discharging the battery module at a current of 180 A, which is known as the 9 C-Rate of discharge. The use of BEVs and PHEVs causes charge/discharge cycles to be very dynamic. The capacity and efficiency of energy storage, and thus the outcomes of the BTMS system, are heavily impacted by the practicability of a protective circuit model with battery system. To ensure accurate voltage and current readings during charge and discharge cycles, all battery modules were required to have an appropriate

safety circuit module. Two Lithium -Ion cells were submersed in molten Phase Change Material at 5, 10, and 15 mm intervals for the parametric experiment. The mass of the PCM is represented by the space between the cells. Given that the aluminium tube has a thickness of 4.76 mm, the bare minimum spacing should be 5 mm. Earlier research has shown that 15 mm is the maximum thickness [17]. In each case, the PCM's mass can be calculated by multiplying its density by the effective volume between the battery cells. A cooling system's ideal operating temperature is determined by the PCM's melting point. As a result, pick a PCM that works for the application carefully. On the other hand, PCMs and composites made of paraffin showed thermal stability, meaning they could be melted and solidified again and again [18]. The present study requires that the battery temperature remain below 50°C. The optimal PCM for cooling was determined to be paraffin C20-C33. Table 4 details all of the PCM's thermo-physical characteristics that are based on paraffin.

Table 4. Characteristics of paraffin

Paraffin	Range
Thermal conduction	0.23 W (mK ⁻¹)
Specific heat capacity	2.385 kJ/ (kg K)
Density (20 °C-solid)	0.913 kg/L
Melting range	48–50 °C
Density (70 °C-liquid)	0.770 kg/L

Fig. 3 shows that the 3/16-inch capillary aluminum tubes meeting ASTM B280 specifications were used to interleave Li-Ion cells. The dimensions of the tubes were 4.8 mm in outside diameter and 0.8 mm in wall thickness. Changing the number of aluminum tubes in the cooling mass caused a change in its thermal conductivity. Paraffin has a thermal conductivity of only 0.2 W/m K, whereas aluminum's value is 386 W/m K. In order to determine the PCC cooling mass's effective thermal conductivity, we utilized equations (1) and (2) in conjunction with citations of previous studies [19]. A suitable space to fill the paraffin was achieved by placing aluminium tubes at equal distances and choosing 3, 5, and 7 tubes, respectively. The 3-,5-, and 7-tube configurations have effective thermal conductivities of 16.3, 25.2, and 35.4 W/m K, correspondingly. Compared to its pure state, PCM's heat conductivity was 171 times higher when seven aluminium tubes were inserted. The study found that compared to pure PCM, the combined thermal conduction of phase change material plus metal was 218 times higher.

$$K_{eff} = (1 - \varepsilon)K_{pcm} + \varepsilon K_{metal} \quad (1)$$

$$\text{Porosity, } \varepsilon = \frac{\text{pore volume}}{\text{total volume}} \quad (2)$$

Where,

K_{pcm} and K_{metal} = Thermal conduction of PCM and metal,

ε = Permeability of the PCM, and

K_{eff} = Effective thermal conductivity.

Capillary aluminium tubes allow water to flow through a PCM cooling mass, making it an ideal coolant for a hybrid cooling mechanism. In order to maintain the water circulation from the reservoir to the capillary aluminum tubes and back again, a 27 L/min pump was employed. The power rating of the pump's was 40 W and it ran at 50 Hz on 100 V. We took extra care not to physically damage the pump by drying it up while it was running. The WFL that was taken into account in this study was found to be between one and two liters per minute [20].

2.1 Acquiring temperature data

Table 5. Details of the thermocouple for measuring temperature

Characteristics	Range
Module	SA1XL-K-SRTC
Type	Type-K
Make	OMEGA
Patch	
span	25 mm
breadth	9.5 mm
Strip	
span	25 mm
thickness	0.001"
width	12.7 mm
leg	
Positive	Chromel (10% Cr and 90% Ni)
Negative	lumel (2% Mg, 1% Si, 2% Al and 95% Ni)
self-adhesive temperature	260 °C
Lead wire	30 AWG fiberglass
paste on temperature	315 °C
Response time	< 0.15 s

The present investigation relied heavily on surface temperature measurements. To measure the temperature, an OMEGA Engineering K-type thermocouple was employed. Table 5 displays the SA1XL-K-SRTC thermocouple specifications. The temperature was recorded using a 'NI 9213' data logger from National Instruments. The NI 9213 has a total of 16 thermocouple channels, including one for cold junction compensation and one for internal auto zero. The voltage measuring range is ± 78.125 mV, and it has a resolution of 24 bits for the analog to digital conversion (ADC). It is compatible with the vast majority of thermocouple types. It has two measuring modes: fast speed and high resolution. The data logger's sensitivity for several types of thermocouples are displayed in Table 6.

Table 6. Sensitivity of data logger temperature measurements

High-speed mode (°C)	
B Type	< 1.1
High-resolution mode (°C)	
R, S Type	< 2.7
J, K, T, E Type	< 0.24
N Type	< 0.34
B, R, S Type	< 0.14
J, K, T, E, N Type	< 0.01

2.2 Electronic DC load

A programmable electronic load, namely the 'IT8514C' model made by ITECH Electronics was utilized to expulsion the batteries at different C-rates in order to determine its discharge temperature. The 'IT9320' software that comes with the electronic load allows to program several discharge modes like constant current (CC), constant resistance (CR), constant wattage (CW), and constant voltage (CV). Table 7 displays the rated input range for the 'IT8514C'.

Table 7. Specified input parameters for IT8514C with direct current load

Factors	Range	
Operating voltage (Min)	0.25 Voltage at 24 A	2.5 V Voltage at 240 A
Input power	1500 W	
voltage input	0 to 120 V	
current input	0 to 24 A	0 to 240 A

3 Design of experiments

The Design of Experiments (DOE) is a powerful tool for creating reliable results from scientific investigations. One major benefit of statistical DOE over the classical engineering method is that it allows for the simultaneous study of multiple process or design variables, providing a more comprehensive understanding of how all of the input variables contribute to the response being measured in the experiment [21]. Using a model equation, one may identify the best process variables, reduce the number of experimental runs, and find the experimental error. Learning the relevance and effect of different design or process variables on performance metrics is another perk. Maximizing a response that is impacted by several variables is the objective of response surface modeling (RSM). To model and analyze such situations, a mathematical and statistical technique was used. Under conditions of high discharge rates, active air cooling fails to maintain a consistent temperature inside a large battery pack [22]. While cooling systems based on pure PCM are good at controlling temperature and dispersing heat uniformly, they reach a breaking point when exposed to maximum C-rates and frequent charge/discharge cycles, at which point the PCM melts. Airflow aided in the removal of latent heat from the PCM cooling mass in the hybrid cooling scenario [23]. Preliminary experiments conducted under Stage-1 also show similar outcomes.

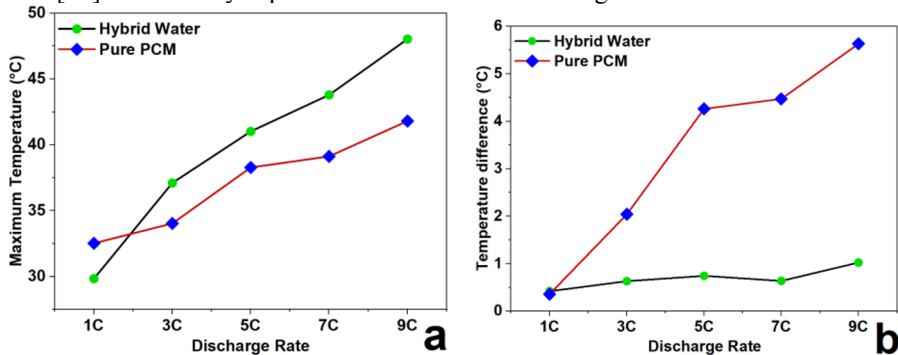


Figure 4. (a) maximal temperature and (b) temperature variation at different discharging rates: temperature design of only PCM and hybridized cooling.

Fig. 4 compares the neat PCM and hybridized cooling systems and displays the maximum temperature and temperature differential. When it comes to controlling temperatures, it seems that neat PCM cooling is better at maximum discharge rates. Nevertheless, hybrid cooling achieves higher temperature uniformity. So, moving forward to Stage-2, our current effort is to build comprehensive factorial design-based regression models for thermal control of hybrid batteries utilizing DOE and RSM. Several plots have been used to study the effects and interactions of each design factor. The results of the pilot testing dictated the settings that were ultimately selected. The number of experimented trials was calculated using a complete factorial DOE that took three factors and three levels into

account [24]. Each Li-Ion battery had two thermocouples, therefore the total temperature reading was actually two separate readings. The total number of experiments, N , is equal to n times L^F , which is 27, as indicated in Table 8. The variables n , L , and F stand for the number of replications, levels, and factors, respectively.

Table 8. Experimental parameters (input and output)

Input factors	Levels	Output response
A	3	Battery temperature
B	3	
C	3	

With 27 distinct sets of variants ($LF = 27$), the evaluation was conducted. With each cycle of the experiment, we recorded the Z and the maximal temperature that the LIB could withstand. It was ensured that the circumstances were identical for both replications by packing two types of batteries with the cooling material and Y in the container. A battery was used with industry-standard stipulations so that it could more easily compare the findings to those of previous research [25]. The temperature and uniformity of the battery are greatly affected by various design aspects of the hybridized cooling system, such as X , Y , the kind of coolant, Z , and the type of PCM. Table 8 shows the levels of the design factors that were considered for the experiments and the linear regressive models. All input parameters linked with low, medium, and high levels were measured depends on the predictable output reaction [26]. For the regression model, the values of the parameters are listed in Table 9. Table 10 display the experimental results.

Table 9. Experimental design of parameters and its levels

Factor Code	Low	Medium	High
A	0.06	0.12	0.18
B	5	8	11
C	1.3	1.6	1.9

Table 10. Experimental Values

S. No.	A - Mass of PCM	B - Thermal conductivity	C - Rate of water flow	Battery temperature
1	0.06	5	1.3	44.89
2	0.06	5	1.6	40.52
3	0.06	5	1.9	36.15
4	0.06	8	1.3	46.35
5	0.06	8	1.6	43.17
6	0.06	8	1.9	39.99
7	0.06	11	1.3	48.03
8	0.06	11	1.6	46.23
9	0.06	11	1.9	44.46
10	0.12	5	1.3	39.58
11	0.12	5	1.6	37.10
12	0.12	5	1.9	34.62
13	0.12	8	1.3	39.92
14	0.12	8	1.6	38.43
15	0.12	8	1.9	36.97
16	0.12	11	1.3	40.32
17	0.12	11	1.6	39.97
18	0.12	11	1.9	39.62

19	0.18	5	1.3	34.28
20	0.18	5	1.6	33.69
21	0.18	5	1.9	33.10
22	0.18	8	1.3	33.50
23	0.18	8	1.6	33.70
24	0.18	8	1.9	33.89
25	0.18	11	1.3	32.61
26	0.18	11	1.6	33.70
27	0.18	11	1.9	34.80

A scaling rate of 3.40 separates the thermal conductivity values from Eq. (1), which are required for the regression equation and graphs. The primary goal of the experiment was to determine the effect of each input parameter and how they interacted with each other on the output parameter [27].

4 Results and discussions

First, statistical analysis determines which factors have a significant impact on the output response and how those factors interact with one another. Then, using tools like surface response and contour plot, it explains how the parameters interact with one another to produce the desired output responses [28]. These parameters can be determined with the use of ANOVA.

4.1 ANOVA

Table 11. Results on ANOVA for output response of battery temperature

Source	DF	Seq SS	Contribution	Adj MS	F-Value	P-Value
X - Mass of PCM	2	415.873	73.96%	207.936	4088.09	0.000
Y - Thermal conductivity	2	37.071	6.59%	18.535	364.41	0.000
Z - Rate of water flow	2	37.210	6.62%	18.605	365.78	0.000
X * Y	4	24.469	4.35%	6.117	120.27	0.000
X * Z	4	33.567	5.97%	8.392	164.99	0.000
Y * Z	4	13.675	2.43%	3.419	67.21	0.000
Error	8	0.407	0.07%	0.051		
Total	26	562.271	100.00%			
S – 0.22553, R ² – 99.93, Adj. R ² – 99.76, Pred. R ² – 99.18						

The impact of control factors on the battery temperature (Temp) was investigated using the DOE tool Minitab® 17. The findings are presented in Table 11 by means of the ANOVA. In order to better comprehend the ANOVA table, please refer to the following definitions. The study's design factors that were considered and had an impact on the response term are the first three terms under the specified source terms; these are known as major effects [29]. The causes of data variance are the first three terms under this heading. When any two strategy factors interact and effect the result term, the outcome is the interaction effect, which is comprised of the following three terms. Seventhly, we factor in the three-dimensional interaction, which considers how each component affects the final answer. We learn about the errors or residuals in the eighth term. Assuming that variances are homogeneous with respect to the sample means and normally distributed is a common error in analysis of variance (ANOVA). "Degrees of freedom" (DoF) stands for the total terms that went into the inaccurate prediction. It is considered that there are one fewer degree of freedom than the quantity of levels (L – 1) in the primary impact [30]. Simply multiplying the domains of

function (DoF) of the terms that are interacting yields the domain of function (DoF) that results from an interaction effect. Subtracting the total number of experimental trials (m minus N) from the number of variation groups compared yields the margin of error (DoF of error). One method to measure the dispersion of the components in the model is the sequential sum of squares, or Seq SS. The mean square (MS) that remains after removing variables that do not contribute to the response equation is referred to as adjusted mean square (Adj MS). As a ratio of corrected MS to residual error, the F-value is computed for hypothesis testing in regression. A high R-squared (R-Sq) value indicates that the data agree well with the fitted regression line, while a low p-value indicates that the evidence measures against the null hypothesis. A maximum R-Sq value (99.93%) derived from the analysis indicates that the data gained during the research have exhibited dependability and correctness. All the components and their interactions had P values higher than the critical threshold ($\alpha = 0.05$), indicating a 5% likelihood of a difference, according to the ANOVA table.

4.2 The regression model

A regression model was created according to the formula in Eq. (3) to examine the correlation between the research-relevant input variables. Assuming certain values for the parameters, the equation's output response can be determined. The input parameters of the regression equation are PCM, PCC, and WFL, as shown in Tables 8 and 9. The output response is determined by the three parameters and their individual and interaction effects, as shown in equation (3). The regression model validates the ANOVA findings by offering a real-world connection between the study variables.

$$\text{Battery Temperature} = 77.363 - 165.37 X - 0.4672 Y - 25.424 Z - 7.926 X*Y + 92.92 X*Z + 1.1852 Y*Z \quad (3)$$

In Fig. 5, the residual plot displays that all of the battery temperature data points are clustered around the optimum-fit line on the normal probability plot. This indicates that the data is reliable and normal by ignoring small deviations. Based on the straight-line distribution of the residuals, researchers can conclude that the errors follow a normal distribution. Also, there was no discernible pattern or out-of-the-ordinary structure in the data as shown by the fits and order charts. The linear, normal, and residues shown in the residual plots validate the regression model and ensure the trustworthiness of the regression analysis

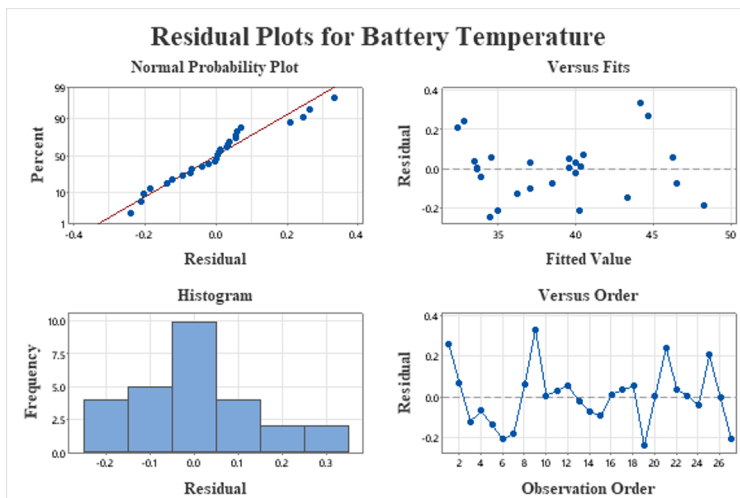


Figure 5. Residual plots for battery temperature.

It appears reasonable to assume that all three parameters have a relatively substantial effect on battery temperature, as seen in the main effect plot in Fig. 6. Nevertheless, the A and C have downward-sloping slopes, suggesting that lower temperatures are associated with higher values. Conversely, a temperature increase may result from the thermal conductivity of the PCC slope that is upwardly sloping, which represents greater values. This is correct since a low paraffin-to-volume ratio is the result of increasing the heat conductivity through the use of more aluminium tubes. Due to the lower temperature at which thermal diffusion occurs between the battery and the paraffin, the battery temperature increases. By balancing the design parameters using optimization, surface, and contour plots, the battery pack's heat management can be optimized. The result is that the Li-Ion cells work better and last longer.

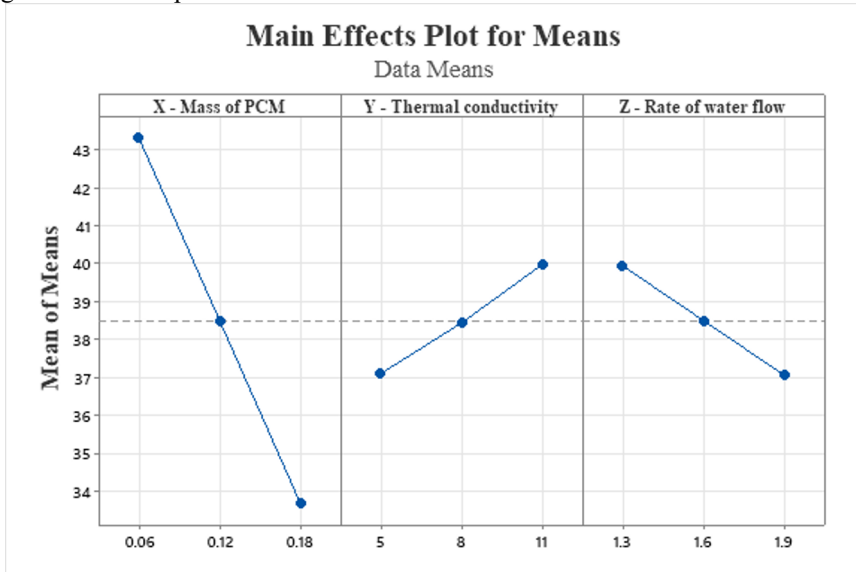


Figure. 6. Battery temperature: main effect plots.

4.3 Response surface methodology

By maintaining the Z parameter at a mean value (the mid-level), contour graphs illustrate the relationship between the battery pack temperature and any two design parameters. In this investigation, we employed WFL, PCC thermal conductivity (as a function of the number of aluminium tubes sandwiched among dual battery cells), and PCM mass (which directly impacts paraffin's heat capacity). The third property, paraffin's heat capacity, allows for heat dispersion from the surface of the battery, while the first two help to dissipate heat from PCM to the atmosphere. Based on the contour plot in Fig. 7(a), it is clear that using a high mass of paraffin and as few as three tubes can obtain a low temperature. Both factors perform best when set to medium levels, though. Fig. 7(b) displays the temperature contour of Y vs Z, demonstrating that a high Z is required for temperature control when the number of aluminum tubes is limited. But a maximum Z isn't ideal because it necessitates powerful pumps and the upkeep of high-pressure connections to circulate water. The graph clearly shows that maintaining medium values for both parameters result in better cooling. Fig. 7(c) shows the correlation between PCM and WFL heat capacities. It demonstrates that a significant decrease in water cooling is possible for PCM with a larger heat capacity. What this means is that there is a lot of room to cut down on pumping effort. Increasing the mass of PCM or choosing the best paraffin will both raise the heat capacity. A simple answer would be to increase the paraffin's bulk. But the battery pack can get bigger and heavier as a result. Low

thermal conductivity is a hallmark of paraffin-based PCM materials, which means they will inevitably fail to remove heat from the cooling mass. A more precise regulation of the battery pack's temperature may be possible with the addition of a water flow channel by the paraffin mass.

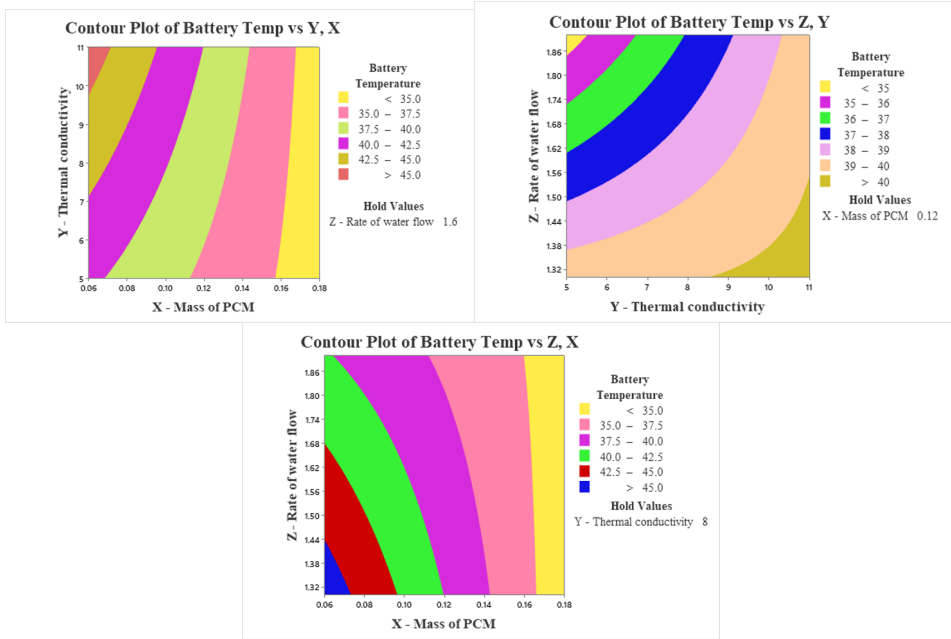
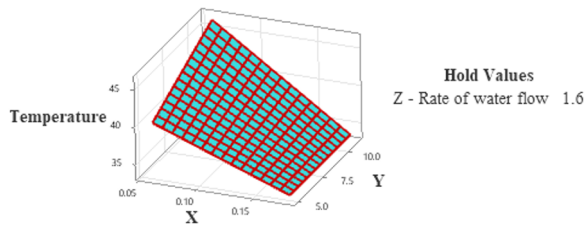


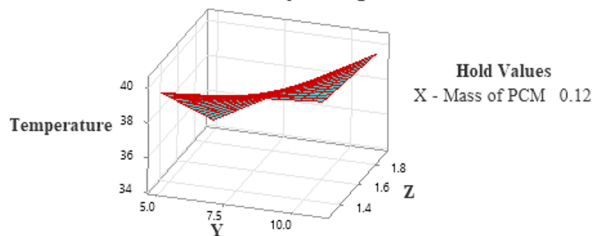
Figure. 7. Contour plot: Battery temperature response of input parameters of (a) X vs Y, (b) Y vs Z and (c) X vs Z

To further comprehend the impact of the interplay between the three elements on the target response, surface plots are an additional useful tool. Fig. 7 shows how the battery pack temperature is affected by all three design parameters.

Surface Plot of Battery Temperature vs Y, X



Surface Plot of Battery Temperature vs Z, Y



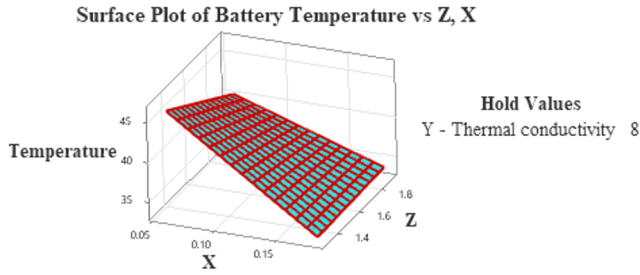


Figure 8. 2D plot: Output response battery temperature of input parameters of (a) X vs Y, (b) Y vs Z and (c) X vs Z

Increasing the factor, A has a significant impact up to a point, as shown in Fig. 8(a), however as the heat capacity rises, X also increases. After a certain point, adding more paraffin to the mix has no discernible impact on the temperature curve, making it appear horizontal. The results are consistent with this occurrence. The graph demonstrates that thermal conductivity has no significant impact on temperature regulation. This study found that the temperature regulation of the battery pack was unaffected by the addition of additional aluminum tubes. Fig. 8(b) shows the correlation between WFL, battery temperature, and the quantity of aluminum tubes. Note that WFL makes use of the same aluminum tubes that conduct heat to channel water flow; increasing the flow rate improves temperature control, but increasing the number of tubes has the opposite impact. The hybrid cooling pack described here relies on a small number of aluminium tubes. Fig. 8(c) shows how the combined heat capacity of PCM and WFL affects the temperature of the battery. These findings corroborate with Fig. 8(a) that compared to WFL, paraffin's heat capacity significantly affects battery temperature. To avoid heat lock, which can happen when the battery is continuously discharged and charged at greater discharge rates, the PCM is cooled using aluminum tubing and running water.

4.4 Regression equation

Table 12. Results obtained by optimizing with different mixes of A, B & C.

Solution	X – Mass of PCM	Y – Thermal conductivity	Z - Rate of water flow	Battery Temperature Fit	Composite Desirability
1	0.18	11	1.3	32.40	1.0000
2	0.18	5	1.9	32.86	0.9840
3	0.164	5	1.9	33.32	0.9538
4	0.18	5	1.3	34.52	0.8762
5	0.18	10.9	1.9	35.00	0.8453

Table 12 displays the battery temperature output values for different combinations of input variables as determined by the statistical model's regression equation (Eq. 3). These numbers help determine the optimal value for each design factor based on the expected output result, since they depict the interaction effect of those parameters. It is feasible to achieve a temperature control of approximately 40°C and 30°C by combining two sets of input parameters, as shown in Table 12, which displays the different combinations for temperature response (Temp). It shows how input parameters need to be carefully selected to provide a lightweight, low-operating-cost, and inexpensive system for any desired controlled temperature. The thermal management system's weight and price tag would go up when the

PCC went up because more aluminium would have to go into the PCM-metal matrix [37]. Also, if PCM were to increase, the battery box's volume would grow, making the thermal management system larger. On the other hand, if WFL were to increase, the cooling system's pumping power would have to climb, it is parasitic in nature. As demonstrated in trial 5 of Table 12, the study achieved a maximum temperature control of 32.40°C by taking the minimum and maximum values of all three design factors. The 0.18 kg mass, 11 W mK⁻¹ thermal conductivity, and 1.3 L min⁻¹ water flow rate are all attributes of the three aluminum tubes that make up the PCM. A mini-channel with a pumping power of 6×10^{-3} W cell⁻¹ and a cross-sectional area of 9 mm² has a flow rate of 1.3 L min⁻¹. Additionally, they foresaw a 20-fold rise in pressure loss for every 1 liter/min increase in flow rate. Thus, the power would grow by a factor of 200 for every one liter of flow rate per minute that is increased. Like the mini-channels, the uses of aluminium tube with a cross section of 8.04 mm². Having said that, the greatest flow rate needed for the current project under 9 C discharge conditions is 2 L/min when PCM is present, which does not necessitate an exorbitant amount of pumping power. Thus, it is essential to manage the amounts of PCM and aluminum when building the hybrid battery pack. A volume gain of 664.32 mm³ and a mass gain of about 6 g/cell would result from increasing the diameter of just one aluminium tube. A module consists of 20 cells and weighs 120 g. An electric vehicle's battery pack would gain 7.2 kg in weight. For PCC purposes, the battery pack just considers the aluminum tube's mass. More pipework to transfer cooling fluid from pump to battery pack is not considered. Therefore, for inexpensive and lightweight battery packs, it is recommended to keep the aluminium tube count low. There are two possible configurations for controlling the temperature within ~40 °C, as shown in Table 12. The second combination achieves the same level of temperature control with fewer aluminum tubes and a lower flow rate than the first one. Excess PCM in the cooling system increases its heat capacity at the expense of some of its heat dissipation, according to the reasoning behind this. In order to maintain a temperature of approximately 30°C, Table 12 suggests two different combinations. Combination 3 is better than Combination 4 since it reduces the mass of an electric vehicle's battery pack by 36 kg, due to its 30 g less PCM per cell. But the flow rate has gone up a little, so you might have to crank up the pump a little bit more.

5 Conclusions

The increased interest in PCM-based cooling can be attributed to its remarkable thermal stability when subjected to repeated solidification and melting processes. To get around the problem of thermal conductivity that comes with using only PCM cooling, a recent trend is to use hybrid cooling systems. The lithium-ion battery cells' suggested hybrid cooling system relies on water, an aluminum housing, aluminium pipes, and a paraffin-based PCM. As it travels through aluminium tubes, water comes into contact with no other material. Because of this, aluminium tubes should not experience corrosion or any kind of degradation or aging effect. The paraffin's stability in both solid and liquid phases is guaranteed by filling the aluminum container that comes into contact with the aluminium tube's exterior with it. No interactions, even at elevated temperatures, are anticipated between paraffin and metals. Because of this, we anticipate that the cooling system will function as intended throughout its useful life. The paraffin material's evaporation temperature is a critical consideration for the suggested cooling system's performance. This study has zeroed in on three critical design aspects that influence the Li-Ion battery pack's temperature control system: the hybrid cooling system. Hybrid cooling outperforms pure PCM cooling at greater discharge rates, according to the temperature uniformity test's preliminary trials. Experiments were conducted and components' influences on the battery's temperature were analyzed using a complete factorial DOE technique. The hybrid cooling system underwent a pioneering

redesign. An analysis of the best way to optimize the electric vehicle's battery pack was conducted using a statistical regression model. Based on the findings, it is evident that:

- The primary determinant of the battery's temperature regulation is the mass of PCM. A higher heat capacity was shown to provide better temperature control with increasing bulk. When the value was above the critical point, however, the temperature control remained unaffected.
- The effect of the PCC's thermal conductivity on the battery's temperature regulation was negligible. Nevertheless, the PCM's thermal conductivity and the coolant flow channel were enhanced by inserting aluminum tubes into it. In hybrid cooling, the number of tubes required to extract the latent heat from the phase change material cooling mass is absolutely minimal.
- The effect of WFL on the control of battery temperature is large. When using greater discharge rates and frequent charge/discharge cycles, pure PCM cooling usually doesn't work, hence water flow becomes critical for dissipating the latent heat of PCM. But when contrasted with paraffin's heat capacity, its impact is negligible.
- The quantity of aluminum tubes and PCM mass would have the most impact on the battery pack's size and weight out of the three hybrid cooling design parameters suggested in this research. Optimal design parameters for minimizing overall battery pack bulk were shown by the regression model from this study when employed.
- A coolant flow rate of no more than 1.3 L/min is required due to the presence of PCM. Therefore, it is not particularly important when considering pumping power. A more adaptable battery pack might be achieved by modifying the coolant type or raising the flow rate beyond 1.3 L/m, both of which would improve heat dissipation. Nevertheless, the system's initial cost and pumping power would be increased.
- The suggested hybrid battery pack can be easily adapted to use either liquid or air cooling, depending on the situation. An alternative to using liquid to cool the battery pack is a hybrid cooling system, which allows drivers to choose between using air through aluminum tubes or liquid.

References

1. G. M. Pradeep, T. Sankaramoorthy, M. Elango, T. N. Kumar, R. Girimurugan, Structural analysis and mechanical properties of thermal battery by flexible phase change materials [PCM]. *Materials Today: Proceedings*. **56**, 3196 (2022).
2. Z. Gao, F. Deng, D. Yan, H. Zhu, Z. An, P. Sun, Thermal performance of thermal management system coupling composite phase change material to water cooling with double s-shaped micro-channels for prismatic lithium-ion battery. *J Energy Storage*. **45**, (2022).
3. Z. Liu, B. Wang, S. Chen, P. Li, Lithium-ion battery pack thermal management under high ambient temperature and cyclic charging-discharging strategy design. *J Energy Storage*. **80**, (2024).
4. N. Napa, M. K. Agrawal, B. Tamma, Phase change material properties identification for the design of efficient thermal management system for cylindrical Lithium-ion battery module. *J Energy Storage*. **99**, (2024).
5. Srilakshmi, Koganti, Sravanthy Gaddameedhi, Subba Reddy Borra, Praveen Kumar Balachandran, Ganesh Prasad Reddy, Aravindhababu Palanivelu, Shitharth Selvarajan. Optimal design of solar/wind/battery and EV fed UPQC for power quality and power

- flow management using enhanced most valuable player algorithm. *Frontiers in Energy Research* **11**, 1342085 (2024).
6. V. Saxena, A. Kumar, A. Sharma, S. K. Sahu, S. I. Kundalwal, Thermal Analysis of a Li-Ion Battery Coupled with Phase Change Material (Paraffin Wax RT-35) filled with Copper Metal Foam: A Numerical Study. in American Society of Mechanical Engineers, Power Division (Publication). *POWER* **4**, (2022).
 7. Murugesan, Palpandian, Prince Winston David, Rajvikram Madurai Elavarasan, G. M. Shafiullah, Praveen Kumar Balachandran. A jigsaw puzzle-based reconfiguration technique for enhancing maximum power in partially shaded hybrid photovoltaic array implementation. In *Green energy systems*. 223 (2023).
 8. N. Napa, M. K. Agrawal, B. Tamma, Design of novel thermal management system for Li-ion battery module using metal matrix based passive cooling method. *J Energy Storage*. **73**, (2023).
 9. C. Kang, J. Yang, X. Yuan, C. Qiu, Y. Cai, A novel multilayer composite structure based battery thermal management system. *Front Energy Res.* **11**, (2023).
 10. Z. Fan, Y. Fu, R. Gao, S. Liu, Investigation on heat transfer enhancement of phase change material for battery thermal energy storage system based on composite triply periodic minimal surface. *J Energy Storage*. **57**, (2023).
 11. Y. Zhang, S. Zhao, T. Zhou, H. Wang, S. Li, Y. Yuan, Z. Ma, J. Wei, X. Zhao, Experimental and Numerical Investigations of a Thermal Management System Using Phase-Change Materials and Forced-Air Cooling for High-Power Li-Ion Battery Packs. *Batteries*. **9**, (2023).
 12. C. Xie, Nano-enhanced phase change material using salt hydrate and cooper nanoparticles for battery thermal management system: Buoyancy-driven approach. *J Energy Storage*. **74**, (2023).
 13. Z. Fan, R. Gao, S. Liu, Thermal conductivity enhancement and thermal saturation elimination designs of battery thermal management system for phase change materials based on triply periodic minimal surface. *Energy*. **259**, (2022).
 14. Ganesan, Sakthivel, Prince Winston David, Pravin Murugesan, Praveen Kumar Balachandran. Solar photovoltaic system performance improvement using a new fault identification technique. *Electric Power Components and Systems*. **52**, 42 (2024).
 15. R. Kumar, A. Mitra, T. Srinivas, Role of nano-additives in the thermal management of lithium-ion batteries: A review. *J Energy Storage*. **48**, (2022).
 16. R. Girimurugan, A. Ranjithkumar, A. Yasminebegum, SK Ahammad, Sameer Ranjan Biswal, G. Ravivarman, Mathanbabu Mariappan, D. Thirumalaikumarasamy. Investigating Electrical, Optical and Structural Characteristics of Cu-Doped TiO₂ Nanostructured Thin Films Synthesized by Innovative Sol-Gel Process. *International Journal of Vehicle Structures & Systems*. **16**, (2024).
 17. A. Mitra, R. Kumar, D. K. Singh, Z. Said, Advances in the improvement of thermal-conductivity of phase change material-based lithium-ion battery thermal management systems: An updated review. *J Energy Storage*. **53**, (2022).
 18. U. Morali, A numerical and statistical study to determine the effect of thermophysical properties of phase change material for lithium-ion battery thermal management. *Numeri Heat Transf A Appl.* (2023).
 19. A. R. Bais, D. G. Subhedar, S. Panchal, Critical thickness of nano-enhanced RT-42 paraffin based battery thermal management system for electric vehicles: A numerical study. *J Energy Storage*. **52**, (2022).

20. Prasanth Ponnusamy, S. Seenivasan, G. Ravivarman, K. Sathiyasekar, Ramasamy Girimurugan, Experimental Analysis of Phase Change Materials Supported with Hemp-Stem-Derived Biochar for Enhanced Solar-Thermal Energy Conversion and Storage. *Engineering Materials for Efficient Energy Storage and Conversion*. 177 (2024).
21. X. Dai, P. Ping, D. Kong, X. Gao, Y. Zhang, G. Wang, R. Peng, Heat transfer enhanced inorganic phase change material compositing carbon nanotubes for battery thermal management and thermal runaway propagation mitigation. *Journal of Energy Chemistry*. **89**, 226 (2024).
22. T. Yang, S. Su, Q. Xin, J. Zeng, H. Zhang, X. Zeng, Xiao, Thermal Management of Lithium-Ion Batteries Based on Honeycomb-Structured Liquid Cooling and Phase Change Materials. *Batteries*. **9**, (2023).
23. L. K. Pratama, S. P. Santosa, T. Dirgantara, D. Widagdo, Design and Numerical Analysis of Electric Vehicle Li-Ion Battery Protections Using Lattice Structure Undergoing Ground Impact. *World Electric Vehicle Journal*. **13**, (2022).
24. Anandha Moorthy Appusamy, Senthil Kumar Laxmanan, Madheswaran Subramaniyan, Pon Maheskumar, K. Suresh Kumar, R. Girimurugan, A Critical Review on Polymer Composites Reinforced with Artificial Fibers Using Fused Deposition Modelling. *J. Environ. Nanotechnol*. **13**, 440 (2024).
25. V.-T. Huynh, K. Chang, S.-W. Lee, One-dimensional and three-dimensional numerical investigations of thermal performance of phase change materials in a lithium-ion battery. *Energies (Basel)*. **14**, (2021).
26. C. Hu, H. Li, Y. Wang, X. Hu, D. Tang, Experimental and numerical investigations of lithium-ion battery thermal management using flat heat pipe and phase change material. *J Energy Storage*. **55**, (2022).
27. A. Dewangan A. K. Shukla, Enhancing Li-Ion Electric Vehicle Battery Performance: Analysis of Advanced Thermal Management Cooling Strategies with Phase Change Material. *Energy Technology*. **5**, (2024).
28. H. Ren, C. Dang, L. Yin, Z. Chen, Optimization research on battery thermal management system based on PCM and mini-channel cooling plates. *Case Studies in Thermal Engineering*. **53**, (2024).
29. Krishnamoorthy, Murugaperumal, S. Devakirubakaran, Arulselvi Ramasamy, and Suresh Srinivasan. "Renewable green hydrogen as a future power for electric vehicles: a perspective." In *Renewable Energy for Plug-In Electric Vehicles*, pp. 95-110. Elsevier, 2024.
30. S. Sudhakaran, M. Terese, Y. Mohan, A. D. Thampi, S. Rani, Influence of various parameters on the cooling performance of battery thermal management systems based on phase change materials. *Appl Therm Eng*. **222**, (2023).